Astron. Astrophys. 354, 1127–1133 (2000)

ASTRONOMY AND ASTROPHYSICS

HC_3N and the ages of dense cores

C. Gwenlan[1], D.P. Ruffle[2], S. Viti[1], T.W. Hartquist[3], and D.A. Williams[1]

[1] Department of Physics and Astronomy, University College London, Gower Street, London, WC1E 6BT, UK
[2] Department of Physics, The Ohio State University, Columbus, Ohio 43210, USA
[3] Department of Physics and Astronomy, University of Leeds, Leeds LS2 9JT, UK

Received 15 October 1999 / Accepted 29 December 1999

Abstract. Fractional abundances of HC_3N and a number of other species are presented for dense core models based on a variety of different assumptions. The highest calculated values of the HC_3N fractional abundances arise in static models where many species striking grain surfaces are processed in hydrogenation reactions leading to the rapid injection of saturated species into the gas phase; in these models the HC_3N is most abundant well before chemical equilibrium is reached. The effects of the various parameters considered are strongly coupled and lead to markedly differing ratios of the HC_3N abundance relative to abundances of other species including H_2CO, C_3H and C_4H. Although none of these models is specific to any particular astronomical object, we briefly compare our results with abundances observed in TMC-1. We conclude that the molecular abundances observed in TMC-1 can be accounted for on the basis of models of the type discussed here, and that - although this much-studied object has unusually high molecular abundances - it is not chemically anomalous compared to other dense cores.

Key words: ISM: clouds – ISM: general – ISM: molecules

1. Introduction

The time dependence of the chemical composition of dark, dense cores provides a potential means of inferring the evolutionary timescales of those sources (e.g. Millar 1990). In particular, the time dependence of the HC_3N to NH_3 abundance ratio at "early times" has received attention, especially in connection with attempts to explain the gradient in that ratio along the TMC-1 ridge (Hirahara et al. 1992; Howe et al. 1996). However, Hartquist et al. (1996) and Ruffle et al. (1997) have stressed that the HC_3N to NH_3 abundance ratio may reflect the extent to which freeze-out onto dust grains has affected the gas phase depletions of elements more massive than helium, rather than provide a reliable chemical clock. Caselli et al. (1998) assumed that the HC_3N fractional abundance is a measure of the depletion, in their observational work on the inference of the fractional ionization in dense cores. As discussed by Hartquist et al. (1996) and, to some extent, by Caselli et al. (1998), there are a variety of ways by which a high HC_3N abundance may arise; in addition to those mentioned above, the "rapid implosion" and "mixing" models are possible explanations. Here we predict the abundances of a number of other species in models giving high HC_3N abundances; our aim is to lay the foundations for observational approaches which will determine which of the scenarios is appropriate.

Sect. 2 contains a description of the various models and a presentation of results. Sect. 3 presents the analysis of the models and Sect. 4 is a discussion of their significance, with some emphasis on TMC-1 for which revised fractional abundances have recently been presented by Ohishi and Kaifu (1998) from new observations. The revised HC_3N abundance is about one order of magnitude larger than derived by Hirahara et al. (1992), and places a significant constraint on the models. It is of interest to assess whether the TMC-1 abundances are anomalously high, compared to other dense cores.

2. Models

The basic chemical network and approach to dynamics are similar to those adopted by Ruffle et al. (1997, 1998, 1999). All hydrogen was assumed to be in H_2 and all other elements were assumed to be in neutral atomic form initially (except for C, S, and Mg which were fully ionized). The UMIST chemical data base (Millar, Farquhar and Willacy 1997) was used. The ambient radiation field adopted was that of Draine (1978) and a cosmic ray induced radiation field (Prasad and Tarafdar 1983) was included.

In some models the number density of hydrogen nuclei, n_H, and visual extinction, A_V, were held constant at 4×10^4 cm^{-3} and 10 magnitudes, respectively. In others, an initial value of n_H (n_{Ho}) and a final value of n_H (n_{Hf}) were specified. In models with $n_{Hf} \neq n_{Ho}$ the density was assumed to increase in a fashion governed by

$$\frac{dn_H}{dt} = B \left(\frac{n_H^4}{n_{Ho}}\right)^{1/3} \left\{ 24\pi\, G m_H\, n_H \left[\left(\frac{n_H}{n_{Ho}}\right)^{1/3} - 1 \right] \right\}^{1/2} \quad (1)$$

where t, B, G, and m_H are the time, a numerical constant, the gravitational constant, and the mass of a hydrogen atom

Table 1. Model Parameters. Number densities are in cm^{-3}, and the notation a(b) signifies a $\times 10^b$. In Column 2 s signifies a static model and c a model undergoing collapse from initial number density n_{Ho} to final number density n_{Hf} according to Eq. (1).

Model		n_{Ho}	n_{Hf}	S	ζ	CO and N_2 freeze-out	Hydrogenation and injection instantaneous
1	s	4(4)	4(4)	0.0	1	No	No
2	s	4(4)	4(4)	0.1	1	Yes	No
3	s	4(4)	4(4)	0.1	1	No	No
4	s	4(4)	4(4)	0.1	10	Yes	No
5	s	4(4)	4(4)	0.1	10	No	No
6	s	4(4)	4(4)	0.1	100	Yes	No
7	s	4(4)	4(4)	0.1	1	Yes	Yes
8	s	4(4)	4(4)	0.1	1	No	Yes
9	s	4(4)	4(4)	0.1	10	No	Yes
10	s	4(4)	4(4)	1.0	1	No	No
11	s	4(4)	4(4)	1.0	10	No	No
12	s	4(4)	4(4)	1.0	1	Yes	Yes
13	c	1(3)	1(5)	0.0	1	No	No
14	c	1(3)	1(5)	0.1	1	Yes	No
15	c	1(3)	1(5)	0.1	1	No	No
16	c	1(3)	1(5)	0.1	10	Yes	No
17	c	1(3)	1(5)	0.1	10	No	No
18	c	1(3)	1(5)	0.1	100	Yes	No
19	c	1(3)	1(5)	0.1	1	Yes	Yes
20	c	1(3)	1(5)	1.0	1	No	No

respectively (e.g. Rawlings et al. 1992). In practice, we took B = 1, which corresponds to a free-fall collapse. In those models,

$$A_V = 0.7 + 1.5 \left(\frac{n_H}{n_{Ho}} \right)^{2/3} \quad (2)$$

in which the constant part is intended to represent the extinction of the ambient medium, while the density dependent part that of the collapsing core. Once n_{Hf} was reached, n_H and A_V were held fixed.

The rate at which collisions between gas phase species and grain surfaces remove species X from the gas phase was taken to be

$$\Gamma_X = 1.1 \times 10^{-17} \mathrm{s}^{-1} m_X^{-1/2} T^{1/2} n_H \; SA \quad (3)$$

where m_X (in a.m.u) and T (K) are the mass of a particle of species X and the temperature, n_H is in cm^{-3}, and

$$A = \begin{array}{l} 1 \qquad (\text{for neutrals}) \\ 1 + \frac{167}{T} (\text{for positive ions}) \end{array} \quad (4)$$

(e.g. Rawlings et al. 1992). S is a free parameter that incorporates uncertainties in this expression associated with the sticking probability per collision, and in the grain size distribution (Draine & Anderson 1985); S = 1 corresponds to the Mathis et al. (1977) grain size distribution, and 100% sticking efficiency.

In all models we set T = 10 K. The cosmic ray ionization rate was taken to be $1.3 \times 10^{-17} \zeta$ s^{-1} where ζ is a free parameter which was assigned values of 1, 10, or 100 in various models.

In some models CO and N_2 were assumed to immediately return unaltered to the gas phase when they struck grains, since these species are amongst those most weakly bound to grain surfaces (cf. Tielens and Allamandola 1987). Furthermore, in some models many species (e.g. O, C, and N) were assumed to be instantaneously hydrogenated to form saturated species (e.g. H_2O, CH_4, and NH_3) which are then injected immediately into the gas phase.

Table 1 gives the parameters defining each of the models for which we give results. The entry in the penultimate column is "No" if CO and N_2 were assumed to return instantaneously to the gas phase. The entry in the final column is "Yes" if prompt injection of saturated hydrogenated species into the gas phase was assumed to occur after a particle of one of a wide variety of reactive species stuck a grain. Models 1–12 are for dark static regions, whereas models 13–20 are for regions undergoing collapse. In all models the initial elemental abundances by number relative to hydrogen were taken to be $7 \times 10^{-2}, 1 \times 10^{-4}, 8 \times 10^{-5}, 2 \times 10^{-4}, 2 \times 10^{-8}, 3 \times 10^{-9}, 2 \times 10^{-7}$, and 7×10^{-9} for helium, carbon, nitrogen, oxygen, sulphur, magnesium, sodium, and silicon, respectively.

Table 2 gives results for the fractional abundances, by number relative to hydrogen nuclei, of HC_3N and several other species at the times at which peaks in the HC_3N fractional abundance occur. An example of the double-peaked behaviour obtained in many models for the HC_3N abundance (Ruffle et al. 1997) is illustrated in Fig. 1, for Model 16. For comparison, the results of Model 12 are shown in Fig. 2. This model represents a static cloud in which freeze–out occurs so efficiently that the second HC_3N peak is suppressed. This second peak is caused by the loss of H_2O and the preferential channelling of C^+ into hydrocarbons. The efficient freeze–out causes nearly all species to be lost from the gas too quickly to allow this second phase chemistry to develop. The times associated with the peaks are given in Table 2; in most (but not all) models the HC_3N abundance shows two peaks, so that two times, t_1 and t_2, are given. The notation x(X) denotes the fractional abundance of species X, $x(\mathrm{X}) \equiv n(\mathrm{X})/n_H$.

3. Analysis

It is of interest to use the results in the table to explore the consequences of the various choices to be made in any particular model. In the work presented here, these choices are (i) static or collapsing cloud; (ii) high or low sticking probability, S; (iii) high or low cosmic ray ionization rate, ζ; (iv) whether or not CO and N_2 are assumed to freeze–out on dust; and (v) whether or not hydrogenation and ejection occur when atoms and radicals arrive at grain surfaces. In this section, we examine the results of models 1–20 to test the effects of these choices, and we do this by examining pairs of models that differ in the single parameter in question.

3.1. Static or collapsing cloud

Models 1 and 13: These are the simplest models in the set, because no freeze–out of any kind is included. The cosmic ray ionization rate has its canonical value. The results show that the

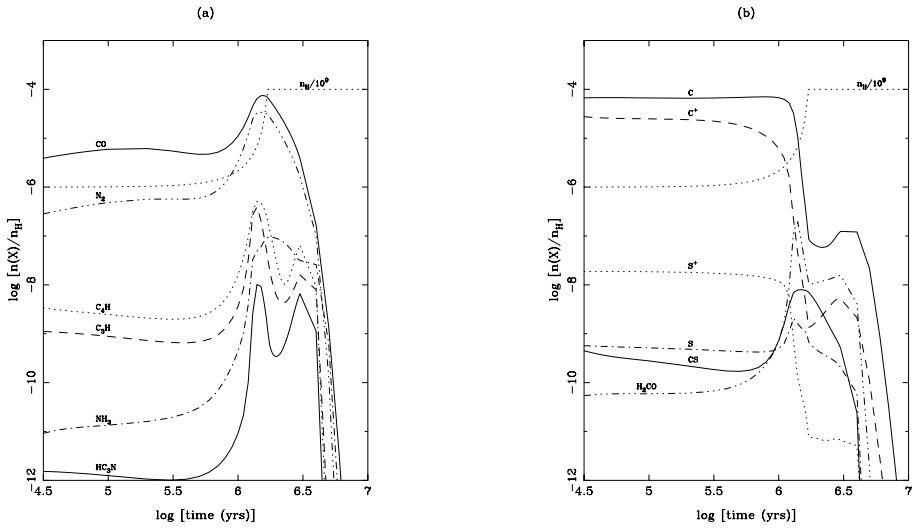

Fig. 1. Fractional abundances of selected species for Model 16, showing the double-peaked behaviour of some hydrocarbons.

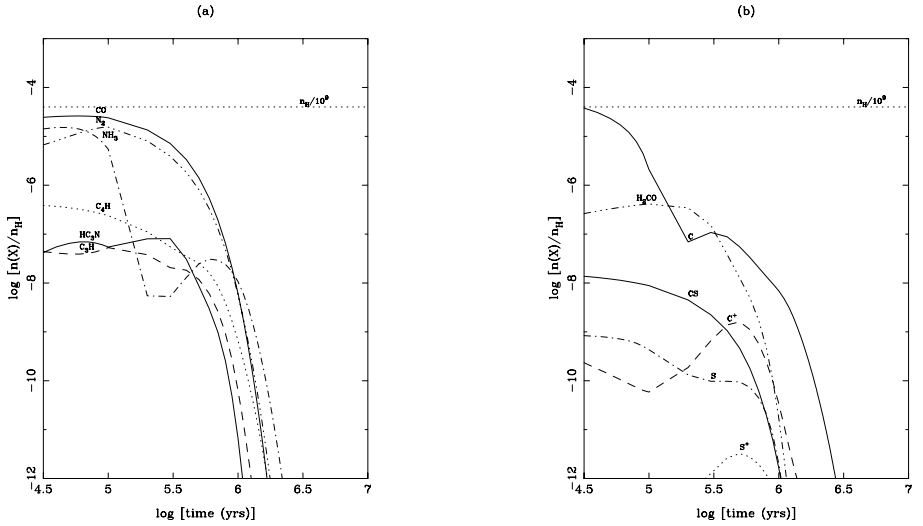

Fig. 2. As in Fig. 1 but for Model 12.

chemistry occurs somewhat later in the collapse case (13) than in the static cloud (1), as expected. The form of the collapse is such that the cloud spends much time at low densities and then rather abruptly moves to high densities. The results for the abundances of molecules are rather similar in these two cases, except for C_3H which is somewhat larger in the collapse case. This may be due to the rather higher density attained in the collapse than used in the static case; this higher density will favour the formation of complex molecules. These two models show no second peak in HC_3N. As discussed previously, the second peak is a consequence of freeze–out, so none is expected here.

Models 2 and 14: These are the next most simple models, with freeze–out but no return of any species; the cosmic ray ionization rate has its canonical value. The value of t_1 is greater for model 14, as expected, but $t_2(2)$ and $t_2(14)$ are similar. As seen for Table 2, the chemistry is also fairly similar for the two models, and we infer that the differences between collapse and static models are unimportant if the value of A_V increases sufficiently rapidly with n_H. The work by Ruffle et al. (1998) showed that too sustained an increase in density with little increase in A_V results in the early-time peak for each of the many complex molecules being small. Consequently, in order for the early-time explanation of the abundances to have some chance of being correct, in this work we have adopted an A_V versus n_H behaviour that results in high early-time abundances for a number of species.

Models 3 and 15: These models are similar to 2 and 14, with the added characteristic that CO and N_2 are assumed not to freeze–out. The results show that t_2 is very long in both models, at 20 My, and this may be unreasonably long when compared with the age of the cloud. The model chemistry takes a long time to produce the maximum HC_3N because N_2 remaining in the gas is a feed-stock for HC_3N production; however, this conversion is recognized to be very slow. The abundances are generally similar for the two models. However, it is noticeable that CS has a different behaviour to that of other species, and at the later time, t_2, is negligible. This is a consequence of freeze–out; while carbon, oxygen and nitrogen are maintained in the gas through CO and N_2, there is no such mechanism for sulphur.

Table 2. Fractional abundances at times t_1 and t_2 when HC_3N peaks occur. The notation a(±b) indicates a $\times 10^b$

Model	t_1, t_2	$x(C_4H)$	$x(HC_3N)$	$x(H_2CO)$	$x(NH_3)$	$x(C_3H)$	$x(CS)$
1	2.0(5)	1.573(-7)	1.825(-9)	2.458(-7)	1.346(-8)	1.566(-8)	1.835(-8)
	-	-	-	-	-	-	-
2	2.0(5)	2.033(-7)	4.549(-9)	3.847(-7)	1.781(-8)	2.301(-8)	1.561(-8)
	5.0(6)	4.111(-8)	6.717(-9)	1.054(-8)	1.249(-8)	1.342(-8)	3.313(-10)
3	2.0(5)	2.035(-7)	4.478(-9)	3.711(-7)	1.709(-8)	2.329(-8)	1.565(-8)
	2.0(7)	3.011(-7)	8.938(-9)	5.542(-8)	3.464(-8)	9.418(-8)	2.926(-14)
4	7.0(4)	5.511(-7)	7.995(-9)	3.997(-7)	4.159(-8)	2.905(-7)	1.608(-8)
	4.0(6)	1.513(-7)	1.295(-8)	1.861(-8)	4.636(-8)	5.084(-8)	4.197(-10)
5	7.0(4)	5.520(-7)	7.843(-9)	3.931(-7)	4.090(-8)	2.899(-7)	1.611(-8)
	9.0(6)	8.746(-7)	1.862(-8)	1.042(-7)	1.042(-7)	2.045(-7)	5.946(-11)
6	3.0(4)	1.128(-6)	1.246(-8)	1.738(-7)	4.833(-8)	4.505(-7)	1.456(-8)
	2.0(6)	5.227(-7)	1.134(-8)	4.942(-8)	8.310(-8)	1.121(-7)	1.636(-9)
7	8.0(5)	1.141(-7)	8.645(-8)	9.686(-8)	9.346(-8)	4.239(-8)	9.719(-9)
	7.0(6)	7.586(-9)	2.849(-10)	2.721(-9)	1.346(-8)	5.285(-10)	3.999(-11)
8	2.0(5)	2.637(-7)	2.560(-8)	6.145(-7)	4.456(-6)	2.177(-8)	1.524(-8)
	6.0(7)	1.124(-7)	8.583(-9)	4.477(-8)	6.336(-8)	2.965(-8)	6.021(-21)
9	6.0(4)	3.541(-7)	5.779(-8)	5.679(-7)	4.508(-8)	3.444(-7)	1.132(-8)
	1.0(6)	3.109(-7)	3.061(-8)	1.319(-7)	9.010(-8)	2.360(-7)	3.049(-11)
10	8.0(4)	1.762(-7)	6.335(-9)	3.218(-7)	8.834(-9)	4.865(-8)	9.534(-9)
	3.0(6)	5.155(-8)	3.170(-9)	2.316(-8)	1.768(-8)	3.162(-8)	1.668(-17)
11	5.0(4)	4.626(-7)	1.642(-8)	5.544(-7)	4.385(-8)	3.784(-7)	1.071(-8)
	9.0(5)	5.105(-7)	1.327(-8)	7.836(-8)	8.335(-8)	1.485(-7)	4.916(-11)
12	3.0(5)	5.526(-8)	8.102(-8)	1.505(-7)	5.278(-9)	2.063(-8)	2.236(-9)
	-	-	-	-	-	-	-
13	1.5(6)	1.642(-7)	2.441(-9)	1.991(-7)	1.860(-8)	9.140(-8)	1.528(-8)
	-	-	-	-	-	-	-
14	1.6(6)	1.378(-7)	3.662(-9)	3.155(-7)	3.173(-8)	7.304(-8)	7.783(-9)
	4.0(6)	1.036(-8)	2.790(-9)	5.644(-9)	7.402(-9)	4.885(-9)	9.309(-10)
15	1.6(6)	1.395(-7)	3.563(-9)	3.067(-7)	3.052(-8)	7.305(-8)	7.339(-10)
	2.0(7)	5.144(-8)	4.960(-9)	2.055(-8)	5.294(-8)	2.438(-8)	1.000(-30)
16	1.4(6)	5.123(-7)	1.017(-8)	1.950(-7)	4.869(-8)	3.920(-7)	7.834(-9)
	3.0(6)	6.494(-8)	6.596(-9)	1.544(-8)	3.155(-8)	1.597(-8)	4.985(-10)
17	1.4(6)	5.193(-7)	9.968(-9)	1.956(-7)	4.852(-8)	3.955(-7)	7.848(-9)
	6.0(6)	5.271(-7)	1.394(-8)	7.231(-8)	8.893(-8)	1.358(-7)	5.115(-12)
18	1.6(6)	3.319(-7)	6.647(-9)	1.008(-7)	8.755(-8)	1.336(-7)	2.786(-9)
	2.7(6)	7.238(-8)	4.971(-9)	2.118(-8)	9.713(-8)	2.293(-8)	2.128(-10)
19	1.6(6)	8.603(-8)	8.238(-9)	5.089(-7)	1.100(-6)	4.494(-8)	6.670(-9)
	4.0(6)	5.165(-10)	8.682(-11)	3.027(-9)	1.513(-8)	2.361(-10)	3.085(-11)
20	1.5(6)	7.898(-9)	2.658(-9)	8.321(-8)	3.909(-8)	4.186(-8)	5.225(-11)
	3.0(6)	8.880(-9)	8.817(-10)	1.089(-8)	2.197(-8)	1.229(-8)	1.000(-30)

Models 5 and 17: These models are similar to Models 3 and 15, but with an enhanced cosmic ray ionization rate, ζ = 10. In both, the second peak at time t_2 arrives fairly late, and the reason is as stated for Models 3 and 15. Results for the molecules listed in Table 2 show that (apart from CS) the abundances are similar at t_1 and t_2, and between Models 5 and 17. This is a result of the rapidity of the gas–phase ion–molecule chemistry, now driven so fast that its timescale is short compared to other important timescales.

Models 6 and 18: These are the counterpart of Models 2 and 14, with a very high cosmic ray ionization rate (ζ = 100). Thus, the chemistry is driven very quickly indeed in the static case (6) to the first HC_3N peak, $t_1(6) = 3\times10^4$ yr. Freeze–out then introduces a second HC_3N peak with generally high abundances. However, these results do not discriminate between Models 6 and 18, for the reasons given in the previous discussion.

Models 7 and 19: These models introduce hydrogenation to Models 2 and 14, and the results show that the effect of the hydrogenation is to enhance H_2CO and NH_3, at the expense of the carbon chains, in Model 19. At peak t_1, there is much more NH_3, while at peak t_2 H_2CO and NH_3 remain high although the other species decline. Hydrogenation provides NH_3 directly, and also the ingredients for H_2CO in H_2O and CH_4. The reason that hydrogenation seems more effective in the collapse phase (19) is that the hydrogenation is most effective in the early, low density phase, during which less carbon and oxygen is tied up in CO.

Models 10 and 20 are like Models 3 and 15, but with the single change to $S = 1$ instead of 0.1. Therefore, the effects of freeze–out should be more pronounced in the results, though, of course, CO and N_2 are retained in the gas phase in these models. The results show $t_2(10) = t_2(20)$ as expected when collisions with grains are more effective as loss mechanisms. However, in these runs, it has been assumed that CO and N_2 do not freeze-out and so these species and the chemistry that they feed have a big effect. Consequently, there is little significant difference between the results of Models 10 and 20.

3.2. High and low sticking probabilities

Much of the description in 3.1 is relevant to the general interpretation of results in Table 2. In this section we make two comparisons to assess the importance of the sticking probability.

Models 3 and 10 are models of static clouds with $\zeta = 1$, retention of CO and N_2 in the gas phase, and no hydrogenation. Model 3 has a small sticking probability, while Model 10 has a large value. As was remarked earlier, $t_2(3)$ is large, because of the recycling of carbon, oxygen and nitrogen. Also, $t_2(10)$ is considerably smaller, and the abundance values at t_2 in Table 2 are generally smaller for Model 10 than for Model 3. This is a consequence of the larger sticking probability in Model 10.

Models 15 and 20 are collapse models with parameters otherwise identical to Models 3 and 10. We see the same behaviour as before with regard to t_2. The more complex species, C_4H and HC_3N, are reduced in Model 20 compared to Model 15, because the recycling of carbon, nitrogen and oxygen from CO and N_2 is limited in scope. It seems, therefore, that the variations in S are masked to some extent by other factors in the reaction scheme.

3.3. The cosmic ray ionization rate

Models 2 and 6 give a comparison of identical static models with low ($\zeta = 1$) and high ($\zeta = 100$) values of the cosmic ray ionization rate, respectively. There are no surprises here. Table 2 shows that $t_1(6)$ is much shorter than $t_1(2)$, because the chemistry is driven much more quickly in Model 6. The abundances of species in Model 6 are generally larger than in Model 2 but by a factor of less than 10, rather than 100, because loss rates are also enhanced at high ζ (cf. Pickles and Williams 1981).

Models 14 and 18 are collapse models otherwise identical to Models 2 and 6. A comparison of molecular abundances for these collapse models leads to the same conclusions as for as the static models.

3.4. Sticking of CO and N_2 to dust

Models 2 and 3 may be used to compare the effects of allowing (2) or preventing (3) this sticking. Although $t_1(2) = t_1(3)$, Table 2 shows that $t_2(3)$ is quite long (possibly unreasonably so, compared with cloud lifetimes) because the extra nitrogen in circulation reacts only slowly though neutral reactions. Over the time $t_2(3)$, HC_3N builds up slowly because of this extra supply of material, compared to Model 2, but only achieves a very slightly enhanced abundance. The CO that in Model 3 remains in the gas is dissociated ultimately by He^+ to C^+ and O, which feed the formation of carbon chains and of formaldehyde. NH_3 is also enhanced, because of the reduction of ions in Model 3 as compared to Model 2. As usual, CS behaves rather differently, because there is no inhibition of sulphur freeze–out; given the long time available in t_2, the loss of sulphur into the dust is near total.

Models 14 and 15 are the counterparts of Models 2 and 3, respectively, for the case of collapsing clouds. In general we find the same kind of behaviour as was described for Models 2 and 3.

3.5. Hydrogenation and instantaneous ejection

Models 2 and 7 are identical static models, apart from the choice of whether hydrogenation products are (7) or are not (2) ejected into the gas. Hydrogenation extends the duration of the chemistry and t_2 is fairly long, for both models. HC_3N at $t_1(7)$ rises to the largest value found in this study. Its abundance is fed by the hydrogenation products NH_3 and CH_4. Its value at $t_1(7)$ is nearly 20 $\times$ larger than at $t_1(2)$. However, not all species behave in the same way, and C_4H is actually larger in Model 2 at time t_1, so the consequences of hydrogenation are rather subtle. NH_3 is a natural consequence of hydrogenation, but the formation of carbon chains is affected by the availability of free carbon. At the later times, t_2, the abundances in Model 7 are much reduced compared to those in Model 2. Thus, although hydrogenation was expected to enrich the chemistry, this is not always the case. In fact, at t_2 the gas has been at high density for such a long time that freeze–out is beginning to reduce most species (though NH_3 still holds out against the trend. It will succumb later).

Models 14 and 19 are collapse models that are in all other respects the counterparts of Models 2 and 7. Again, we see that at the first peak the carbon chains are not enhanced by hydrogenation, but NH_3 and H_2CO are considerably enhanced. At the second peak, the results are as described for the corresponding static models.

3.6. Summary of the analysis

Insofar as general conclusions can be reached, the main point is that the effects of the various mechanisms are strongly coupled, because the timescales associated with them may often be similar. Consequently, the anticipated effects of a particular parameter change are not always found. For example, increasing the cosmic ray ionization rate can increase the destruction rate as well as the formation rate of a particular species. Differential effects in freeze–out, caused by the different thermal speeds of different species (as in the case of H_2O), can cause some species (e.g. hydrocarbons) to rise in abundance for the second peak. The retention of CO and N_2 in the gas phase (on the very reasonable assumption that they bind very weakly to dust grains) offer the possibility that these species, after reaction

Table 3. Timescales of relevance to the chemistry in dark clouds. n_H is the number density of hydrogen nuclei in all forms; S is the sticking probability; ζ is the cosmic ray ionization rate; D is the factor less than unity (typically 10^{-1}–10^{-2}) by which abundances of heavy atoms are depleted by freeze–out.

Collapse	$\sim 10^8/n_H^{1/2}$ yr
Freeze–out	$\sim 10^9/(Sn_H)$ yr
Ion–molecule chemistry	$\sim 10^5(3\times10^{-17}\mathrm{s}^{-1}/\zeta)$ yr
Recirculation time (for CO, N_2, etc)	$\sim 10^5(D/0.1)(3\times10^{-17}\mathrm{s}^{-1}D/\zeta)$ yr

Table 4. Comparison of fractional abundances deduced from the observations of Ohishi and Kaifu (1998) with those from several models giving high values of HC_3N. The computed results are at time t_1.

	HC_3N	H_2CO	NH_3	C_3H	CS
Observations	6.0(-8)	5.0(-8)	2.0(-8)	1.5(-8)	7.0(-9)
Model 7	8.6(-8)	9.7(-8)	9.3(-8)	4.2(-8)	9.7(-9)
Model 8	2.6(-8)	6.1(-7)	4.4(-6)	2.1(-8)	1.5(-8)
Model 9	5.8(-8)	5.7(-7)	4.5(-8)	3.4(-7)	1.1(-8)
Model 12	8.1(-8)	1.5(-7)	5.3(-9)	2.1(-8)	2.2(-9)

with He^+, will provide a source of the main atoms and enrich the chemistry; but the time required for this may be so long that the freeze–out of other species becomes a dominant sink and the expected enhancements do not occur.

The timescales relevant to the present discussion are listed in Table 3. All the arguments made in this section are essentially examples of the conflicting processes, as represented by these timescales. For example, the separation in time between the two HC_3N peaks is determined by the timescale for ion–molecule reactions (setting up the first peak) and the timescale for freeze–out which sets up conditions that may allow the second peak to arise. Other effects, for example the inhibition of CO and N_2 freeze–out so that they remain a 'feed-stock' for second–phase chemistry, also affect these conclusions. On the other hand, the depth of the trough is uninteresting because the trough abundances of various species, such as HC_3N, are just too low to account for the observational data for most sources.

4. Discussion and conclusion

None of these models is specific to any particular astronomical object. They are intended to indicate the relative importance of the various physical and chemical processes involved. Nevertheless, it is also instructive to compare our results with the object that has been most intensively studied, TMC-1. Ohishi and Kaifu (1998) give the most recent abundance determinations. However, our models have not been adjusted for TMC-1; for example, the observationally-determined density in TMC-1 is higher than the value adopted in our static models, and even higher than the final density of our collapse models (Hirahara et al 1992).

One of the highest computed values of $x(HC_3N)$ arises in Model 12, which is one that has the largest adopted value of S and in which atomic carbon striking the grain surface is assumed to be processed to form CH_4 that is quickly injected into the gas phase. For this large value of S a significant fraction of the carbon is contained in gas phase CH_4 before much CO is formed. In this case, the production of trace species is initiated by the reaction of H_3^+ with saturated hydrogenated molecules to form saturated ions which dissociatively recombine, sometimes to form radicals; the reaction of radicals with saturated hydrogenated ions triggers the formation of complex molecules. Other models (7, 8, 9) with constant density and with instantaneous hydrogenation and injection into the gas phase have large peak values of $x(HC_3N)$, roughly comparable to that measured in core D of TMC-1 by Ohishi and Kaifu (1998).

Model 19 with instantaneous hydrogenation and injection into the gas phase but time-dependent n_H does not have such extremely high values of $x(HC_3N)$. This suggests that shock-driven implosion (cf. Hartquist et al. 1996) and chemical youth may be necessary for the highest measured $x(HC_3N)$ values to be produced. In general, the dissociation induced by photons of external origin somewhat suppresses the "early-time" peaks in $x(HC_3N)$.

In Table 4, the observed TMC-1 abundances for several species are compared with results from those models (7, 8, 9, and 12) which seem to give reasonable agreement for HC_3N. Of course, one should not take this comparison too far, for the reasons given at the start of this section, but the table indicates that TMC-1 can be reasonably described by models investigated here. Table 4 indicates that the hydrogenation model used here may be somewhat too efficient in producing NH_3 and (indirectly) H_2CO. The combination of a high cosmic ray ionization rate and efficient hydrogenation leads to significant overproduction of some species. However, an important conclusion to be drawn from an inspection of Table 4 is that TMC-1 need not be considered as an anomaly. Its chemistry can be described satisfactorily by models of the type presented here.

Of the models not incorporating instantaneous hydrogenation and injection into the gas phase, those with ζ = 10 and ζ = 100 are amongst the models with the highest peak values of $x(HC_3N)$. This is of particular interest as Caselli et al. (1998) have concluded that in core D of TMC-1 ζ is of order 100. However, our results indicate that a high cosmic ray ionization rate alone cannot account for the high abundances detected in TMC-1.

In each of many models, the late-time peak in $x(HC_3N)$ associated with depletion is higher than the early-time peak. Hence, it is clear that depletion-enhanced late-time chemistry remains a viable explanation for the high values of $x(HC_3N)$ measured for some dense cores.

Recently Willacy and Millar (1998) noted that Ruffle et al (1997) used a slower accretion rate than is employed in their models, and predicted that this slower accretion coupled with higher values for the sticking coefficient, S, would suppress the double peaked behaviour for H_3CN. In this work, we have shown that suitably high values for S (1.0), as employed in Model 12, does indeed lead to the late–time peaks being re-

moved. However, we note that this result is sensitive to the parameters used; the inclusion of even limited desorption pathways (of CO and N_2) gives rise to double peaked behaviour, as seen in Models 10, 11 and 20.

The results in Table 2 suggest some observational studies that would help identify which of the possible explanations for a high value of $x(HC_3N)$ is most viable for a particular given dense core. If an "early-time", "instantaneous hydrogenation-injection" explanation is appropriate, the ratios of the abundance of HC_3N to each of the abundances of C_4H, H_2CO, and C_3H are considerably higher than if one of the other explanations for a high value of $x(HC_3N)$ is applicable. In other models in which the high value of $x(HC_3N)$ is a consequence of chemical youth, the ratio of the abundance of HC_3N to the abundances of these other species is lower than it is in models in which depletion plays an important role. However, those ratios are considerably smaller in the models in which depletion is important than they are in those in which early-time effects and instantaneous hydrogenation and injection have major consequences.

Acknowledgements. We are grateful to the referee for comments which helped to improve an earlier version of this paper. DAW and SV acknowledge with thanks the support of PPARC. DPR wishes to thank the National Science Foundation (Division of Astronomical Sciences) for support.

References

Caselli P., Walmsley C.M., Terzieva R., Herbst E., 1998, ApJ 499, 234
Draine B.T., 1978, ApJ 36, 395
Draine B.T., Anderson N., 1985, ApJ 292, 494
Hartquist T.W., Williams D.A., Caselli P., 1996, Ap&SS 238, 303
Hirahara Y., Suzuki H., Yamamoto S., et al., 1992, ApJ 394, 539
Howe D.A., Taylor S.D., Williams D.A., 1996, MNRAS 279, 143
Mathis J.S., Rumpl W., Nordsieck K.H., 1977, ApJ 217, 425
Millar T.J., 1990, In: Hartquist T.W. (ed.) Molecular Astrophysics – A Volume Honouring Alexander Dalgarno. Cambridge, Cambridge University Press, p. 114
Millar T.J., Farquhar P.R.A., Willacy K., 1997, A&A 121, 139
Ohishi M., Kaifu J., 1998, Faraday Disc. 109, 205
Pickles J.B., Williams D.A., 1981, MNRAS 197, 429
Prasad S.S., Tarafdar S.P., 1983, ApJ 267, 603
Rawlings J.M.C., Hartquist T.W., Menten K.M., Williams D.A., 1992, MNRAS, 255, 471
Ruffle D.P., Hartquist T.W., Caselli P., Williams D.A., 1999, MNRAS 306, 691
Ruffle D.P., Hartquist T.W., Rawlings J.M.C., Williams D.A., 1998, A&A 334, 678
Ruffle D.P., Hartquist T.W., Taylor S.D., Williams D.A., 1997, MNRAS 291, 235
Tielens A.G.G.M., Allamandola L.J., 1987, In: Hollenbach D.J., Thronson H.A. (eds.) Interstellar Processes. D. Reidel Publishing Company, p. 397
Willacy K., Millar T.J., 1998, MNRAS 298, 562